

# Cyclic Delay Diversity with Index Modulation for Green Internet of Things

Wen, Maiwen; Lin, Shaoe; Kim, Kyeong Jin; Li, Fei

TR2021-077 July 12, 2021

## Abstract

Cyclic delay diversity (CDD) is a simple and yet effective transmit diversity technique. Thanks to its strong power saving capability, CDD is very promising for green Internet of Things (IoT) networks. However, the reduced degrees of freedom in data transmission and the overhead of cyclic prefix lead to unsatisfactory spectral efficiency (SE), hindering the direct application of CDD to IoT networks where short-packet communication prevails. To tackle this problem, in this paper, we propose to convey additional information via the varying cyclic delays for improving the SE of the CDD system based on the concept of index modulation (IM), which applies to both OFDM and cyclic-prefixed single-carrier (CPSC) signals. The methods to generate all possible cyclic delays and the optimal receivers are designed for both proposed systems. To aim at low computational complexity, we further propose a suboptimal receiver for the CDD-CPSC-IM system. Moreover, a closed-form upper bound on the bit error rate (BER) of the CDD-OFDM-IM system is derived, from which the coding gain is characterized. Simulation results in terms of BER corroborate the analysis and the superiority of the proposed systems over the pure CDD-OFDM and CDD-CPSC systems, uncovering the potential of CDD in the application to green IoT networks.

*IEEE Transactions on Green Communications and Networking*



# Cyclic Delay Diversity with Index Modulation for Green Internet of Things

Miaowen Wen, *Senior Member, IEEE*, Shaoe Lin, Kyeong Jin Kim, *Senior Member, IEEE*,  
and Fei Ji, *Member, IEEE*

**Abstract**—Cyclic delay diversity (CDD) is a simple and yet effective transmit diversity technique. Thanks to its strong power saving capability, CDD is very promising for green Internet of Things (IoT) networks. However, the reduced degrees of freedom in data transmission and the overhead of cyclic prefix lead to unsatisfactory spectral efficiency (SE), hindering the direct application of CDD to IoT networks where short-packet communication prevails. To tackle this problem, in this paper, we propose to convey additional information via the varying cyclic delays for improving the SE of the CDD system based on the concept of index modulation (IM), which applies to both OFDM and cyclic-prefixed single-carrier (CPSC) signals. The methods to generate all possible cyclic delays and the optimal receivers are designed for both proposed systems. To aim at low computational complexity, we further propose a suboptimal receiver for the CDD-CPSC-IM system. Moreover, a closed-form upper bound on the bit error rate (BER) of the CDD-OFDM-IM system is derived, from which the coding gain is characterized. Simulation results in terms of BER corroborate the analysis and the superiority of the proposed systems over the pure CDD-OFDM and CDD-CPSC systems, uncovering the potential of CDD in the application to green IoT networks.

**Index Terms**—Cyclic delay diversity (CDD), index modulation (IM), OFDM, single-carrier, permutation.

## I. INTRODUCTION

CYCLIC DELAY DIVERSITY (CDD) [1] is a simple and yet effective technique to achieve transmit diversity that is scalable with the number of transmit antennas without altering the receiver. Owing to its advantages, CDD has been incorporated in the existing standards, such as IEEE 802.11ac, IEEE 802.11n, and Long-Term Evolution (LTE) [2]. CDD was first proposed for orthogonal frequency division multiplexing (OFDM) configurations [1]. It artificially inserts virtual echoes into the effective channel to increase frequency selectivity by transmitting the same OFDM signal from multiple antennas with different delays, which are done in a cyclic manner such that no extension of the guard interval is required to avoid inter-symbol interference (ISI). The use of CDD essentially transforms the spatial diversity into additional frequency diversity from the neighboring subcarriers, which are less correlated or even uncorrelated. Such property facilitates designs of a simple and yet efficient channel estimation scheme by

partitioning the neighboring subcarriers into sets [3], and a differential modulation scheme that operates across the sets to avoid the investment of more pilots to channel estimation due to the reduced coherence bandwidth [4]. Moreover, thanks to the diversity transformation, full diversity over multipath fading channels that is a combination of full spatial and frequency diversity can be achieved either from a space-time coding point of view based on the design criteria derived for space-time block codes [5] or by forward error control (FEC) codes with a special frequency interleaving scheme and multiple access strategy [6]. Specifically, for the latter, the spatial diversity is exploited by channel coding over a set of uncorrelated neighboring subcarriers while the frequency diversity is obtained by distributing the sets over the entire bandwidth.

CDD is favorable for cyclic-prefixed single-carrier (CPSC) block transmission as unlike CDD-OFDM, CDD-CPSC can harvest frequency diversity without FEC coding thanks to the inherent coding across the band in SC systems [7]–[9]. For CDD-CPSC, while the zero-forcing (ZF) receiver fails to pick up any diversity gain, a simple minimum mean-square error (MMSE) equalization can result in differing diversity orders depending on the system parameters [7], as pure CPSC without CDD [10]. Particularly, below a certain data rate threshold full diversity is available to CDD-CPSC with the MMSE receiver, although the diversity may diminish at higher rates. The loss of diversity gains (at higher rates) is caused by the noise and/or ISI enhancement for a linear frequency-domain equalizer. To achieve no loss, and hence the maximum diversity gain at full rate, non-linear equalizers, such as the block iterative generalized decision feedback equalizer [8] and frequency-domain Turbo equalizer [9], have been designed. Recently, the concept of CDD has been transplanted to distributed antenna systems, where the geographically separated single-antenna transmitters cooperate to form virtual CDD-CPSC [2], [11], [13]. The maximum diversity order of such distributed CDD system over frequency-selective fading channels that is equal to the product of the numbers of transmitters and multipath components is proved to be achievable at full rate [2]. Distributed CDD has gained much success in a wide range of applications, including spectrum sharing [11], security communications [12], etc. More recently, distributed CDD has been further extended to distributed asynchronous CDD without requiring a tight synchronization among the spatially distributed nodes [13].

Most of the above mentioned works on CDD-OFDM/CPSC have concentrated on designing schemes to extract the maximum diversity gain. However, maximizing the diversity gain

M. Wen, S. Lin, and F. Ji are with the School of Electronic and Information Engineering, South China University of Technology, Guangzhou 510641, China (e-mail: eemwwen@scut.edu.cn; eeshe.lin@mail.scut.edu.cn; eefeiji@scut.edu.cn).

K.-J. Kim is with the Mitsubishi Electric Research Laboratories (MERL), Cambridge, MA 02139 USA (e-mail: kkim@merl.com).

may lead to a reduction of spectral efficiency (SE) [14]. How to improve the SE while keeping the CDD-OFDM/CPSC framework unchanged for standard conformability is thereby an intriguing and challenging problem, especially for Internet of Things (IoT) networks with short-packet communications, where the CP occupies non-negligible bandwidth resource. To solve this problem, we are motivated by the concept of the recently emerging index modulation (IM) [15]–[20]. Here, IM refers to a class of digital modulation techniques that leverage upon the on-off state of the transmission entities such as antenna, signal constellation, spreading code, and subcarrier to convey information, which has been widely acknowledged as a competitive candidate for next-generation wireless networks [15], [18], [21]. Our idea is to encode the cyclic delays of all transmit antennas for conveying additional information based on the IM concept, where different delays are created from two basic operations: delay permutation and delay shift. This means that the antenna specific delays will be no longer fixed as usual, but allowed to vary with random bits, leading to an SE improvement.

#### A. Related Works

Using permutation as a means to convey information has a history of more than 50 years [20]. In 1965, the first attempt, called permutation modulation (PM), was made by permuting the order of a set of numbers to generate transmission codewords [22]. In fact, many recently proposed IM schemes, including the famous spatial modulation [23], subcarrier index modulation [24]–[26], differential spatial modulation [27], and beamspace modulation [28], happen to follow the basic permutation structure of PM [20]. More recently, the IM concept has been exported to the permutation of diverse signal constellations for OFDM transmission, which is referred to as multiple-mode (MM-)OFDM-IM in [29]–[31]. In [29] and [30], the guidelines for optimizing the performance of MM-OFDM-IM were designed for supporting identical and non-identical cardinalities of the signal constellations, respectively, and the key is to ensure all signal constellations are as distinguishable as possible. Nevertheless, to the best of our knowledge, the PM or IM concept has not been developed and applied to CDD systems with the objective of improving the SE in the literature.

For the design of CDD systems including both CDD-OFDM and (distributed) CDD-CPSC, a great deal of attention has been previously paid to the choice of cyclic delays. There were several considerations for the delay selection, including maximizing the frequency selectivity [5]–[7], [9], removing ISI [13], facilitating channel estimation [13], and improving data rate [33]. Usually, the maximum cyclic delay is preferred as it results in the least overlap between the channel taps from different antennas, and a transformation of spatial diversity into the neighboring subcarriers [2], [6], [9]. However, no matter which choice of cyclic delays is adopted, the cyclic delays of all transmit antennas are always invariant during communications, and they do not carry any information. It is worthy noting that only the work of [7] has concerned permutations of the cyclic delays. However, its purpose is

merely to pick out those candidates of cyclic delays ensuring the exploitation of the full diversity.

#### B. Contribution

In contrast to existing works, our main contributions include the following.

- We propose to index the cyclic delays of all transmit antennas for improving the SE of the CDD system, which applies to both OFDM and CPSC signals yielding the so-called CDD-OFDM-IM and CDD-CPSC-IM, respectively, in this paper. The diverse approaches of creating all possible cyclic delays for CDD-OFDM-IM and CDD-CPSC-IM are respectively designed, which basically contain delay permutation and delay shift operations. In the design, the maximum frequency selectivity and distinguishable effective channels serve as the criteria to attain the advantages of both CDD and IM. The SE improvement achieved by the CDD-OFDM-IM and CDD-CPSC-IM systems is further characterized.
- The optimal receivers based on the maximum-likelihood (ML) criterion are designed for both CDD-OFDM-IM and CDD-CPSC-IM systems. To reduce the high computational complexity of the optimal ML detection due to the involved multiple fast Fourier transform (FFT) operations, we further propose a symbol-wise low-complexity receiver for the CDD-CPSC-IM system, which detects the IM and symbol bits sequentially. Moreover, an upper bound on the BER of the CDD-OFDM-IM system is derived in closed-form, from which the coding gain is further characterized.
- Extensive Monte Carlo computer simulations are conducted to investigate the performance of the CDD-OFDM-IM and CDD-CPSC-IM systems, and the impact of system parameters in terms of uncoded BER. The pure CDD-OFDM and CDD-CPSC schemes without IM are taken as benchmark schemes for comparison. Simulation results corroborate the analysis and the superiority of the proposed schemes over the benchmarks. It is also shown that significant signal-to-noise ratio (SNR) gains can be attained by the proposed schemes for short-packet communications.

#### C. Organization

The rest of this paper is organized as follows. Section II describes the transceiver frameworks of CDD-OFDM-IM and CDD-CPSC-IM. The methods of generating cyclic delay candidates for CDD-OFDM-IM and CDD-CPSC-IM are detailed in Section III. Section IV designs the optimal ML receivers for both CDD-OFDM-IM and CDD-CPSC-IM, and low-complexity suboptimal receiver for CDD-CPSC-IM. Then, the BER upper bounds on both systems are derived and the corresponding BER asymptotic performance is characterized. Simulation results are presented and discussed in Section V. Finally, Section VI concludes the paper.

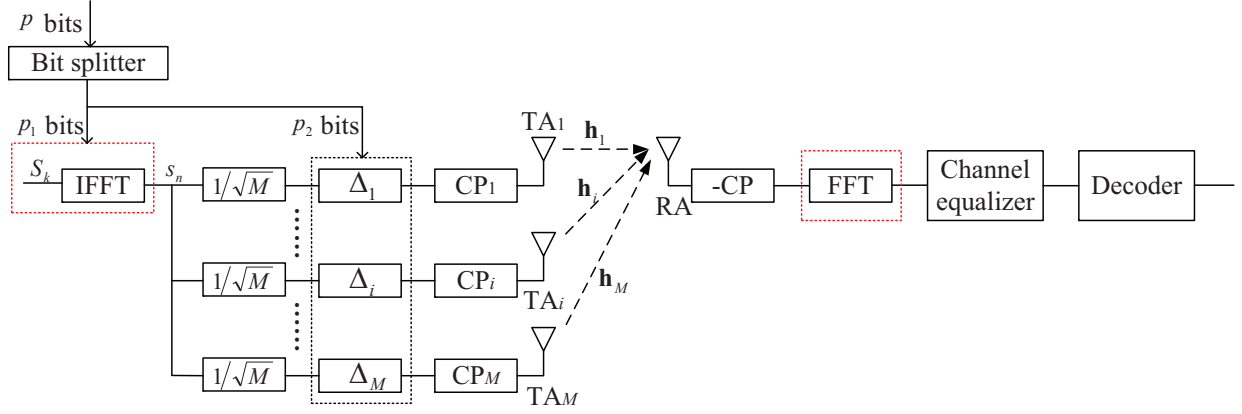


Fig. 1. Block diagram of the transmitter and receiver which operate according to an OFDM transmission scheme, wherein the transmitter transmits additional information using cyclic delay permutation. When using a CPSC transmission scheme, the IFFT and FFT operations in the red dashed boxes need to be removed.

#### D. Notation

Upper and lower case boldface letters denote matrices and column vectors, respectively.  $(\cdot)^T$ ,  $(\cdot)^H$ , and  $(\cdot)^{-1}$  represent transpose, Hermitian transpose, and inversion operations, respectively.  $\|\cdot\|$  denotes the Euclidean norm of a vector.  $\lfloor \cdot \rfloor$  denotes the floor function that returns the largest integer less than or equal to the argument.  $\text{diag}(\cdot)$  defines the forming function used to reshape the vector into a diagonal matrix.  $\mathbf{I}_N$  denotes an  $N \times N$  identity matrix.  $\mathbf{1}_{n \times m}$  and  $\mathbf{0}_{n \times m}$  denote all-one and all-zero matrices of size  $n \times m$ , respectively.  $\text{rank}(\cdot)$  denotes the matrix rank.  $\min\{\cdot, \cdot\}$  and  $\max\{\cdot, \cdot\}$  return the largest and smallest numbers between the arguments, respectively.  $P\{X\}$  denotes the probability of the event  $X$ .  $\mathcal{CN}(\boldsymbol{\mu}, \boldsymbol{\Sigma})$  denotes the distribution of a circularly symmetric complex Gaussian random vector with covariance matrix  $\boldsymbol{\Sigma}$  and mean  $\boldsymbol{\mu}$ .  $\mathbb{E}_X\{\cdot\}$  denotes the expectation over the random variable  $X$ .

## II. TRANSCIVER FRAMEWORKS OF CDD-OFDM-IM AND CDD-CPSC-IM SYSTEMS

In this section, we first consider an OFDM transmission scheme operating over frequency-selective Rayleigh fading channels. The transceiver frameworks of CDD-OFDM-IM and CDD-CPSC-IM systems are given in Fig. 1, in which the inverse fast Fourier transform (IFFT) and FFT operations in the red dashed boxes need to be removed when applying to CPSC signals. Let  $M$  represent the number of transmit antennas (TAs), denoted by  $\text{TA}i$  with  $i = 1, 2, \dots, M$ . The channel from  $\text{TA}i$  to the receive antenna is described by the channel impulse response (CIR)  $\mathbf{h}_i = [h_i(1), h_i(2), \dots, h_i(L_i)]^T \sim \mathcal{CN}(\mathbf{0}_{L_i \times 1}, \frac{1}{L_i} \mathbf{I}_{L_i})$  with a delay spread of  $L_i$  taps in the time domain. We assume that the transmit antennas are placed sufficiently apart such that the channels  $\mathbf{h}_i$ 's are individually independent fading. Moreover, we assume that the channels  $\mathbf{h}_i$ 's remain constant during the transmission of one OFDM block and the number of samples in the cyclic prefix (CP), denoted by  $L$ , is not less than the maximum delay spread of all the channels to avoid ISI, i.e.,  $L \geq \max\{L_1, L_2, \dots, L_M\}$ .

#### A. Conventional CDD-OFDM

At the transmitter, a block of  $N$  frequency-domain symbols, denoted by  $\mathbf{x}_F \triangleq [S_1, S_2, \dots, S_N]^T$ , is first converted into the time-domain version, denoted by  $\mathbf{x}_T \triangleq [s_1, s_2, \dots, s_N]^T$ , via an  $N$ -point IFFT. In the conventional CDD-OFDM scheme, the first TA transmits the data block  $\mathbf{x}_T$  with no time delay, i.e.,  $\Delta_1 = 0$ , and  $\text{TA}i$  with  $i = 2, 3, \dots, M$  transmit different cyclically delayed versions of the vector  $\mathbf{x}_T$ . The cyclic delay in each antenna path can be expressed by

$$\Delta_i = \Delta(i-1), i = 1, 2, \dots, M \quad (1)$$

where  $\Delta$  is the delay spacing measured in terms of the number of sample points with  $1 \leq \Delta \leq \frac{N-1}{M-1}$ . Let  $\mathbf{x}_T(\Delta_i)$  denote the vector  $\mathbf{x}_T$  cyclically shifted by a number of positions  $\Delta_i$ , which can be expressed by

$$\mathbf{x}_T(\Delta_i) = \begin{cases} \mathbf{x}_T, & \Delta_i = 0 \\ \mathbf{P}_N^{\Delta_i} \mathbf{x}_T, & \Delta_i > 0 \end{cases} \quad (2)$$

where  $\mathbf{P}_N^{\Delta_i}$  is the  $\Delta_i$ -th power of the cyclic permutation matrix  $\mathbf{P}_N$  given by

$$\mathbf{P}_N = \begin{bmatrix} \mathbf{0}_{1 \times (N-1)} & 1 \\ \mathbf{I}_{N-1} & \mathbf{0}_{(N-1) \times 1} \end{bmatrix}. \quad (3)$$

Then, each cyclically delayed copy  $\mathbf{x}_T(\Delta_i)$  is appended by the corresponding CP and transmitted from  $\text{TA}i$ . At the receiver, after removing the CP and performing the  $N$ -point FFT, the received block in the frequency domain is given by

$$\mathbf{y}_F = \sum_{i=1}^M \mathbf{X}_i \mathbf{h}_{F,i} + \mathbf{n}_F \quad (4)$$

where  $\mathbf{X}_i = \text{diag}(\mathbf{x}_{F,i})$  is the diagonal matrix of the OFDM block transmitted by  $\text{TA}i$  (i.e.,  $\mathbf{x}_{F,i}$ ),  $\mathbf{n}_F \sim \mathcal{CN}(\mathbf{0}_{N \times 1}, N_0 \mathbf{I}_N)$  is the noise samples in the frequency domain, and  $\mathbf{h}_{F,i} = \mathbf{F}_N \mathbf{h}_i^0$  is the channel frequency response (CFR) of the corresponding path:  $\mathbf{F}_N$  is the  $N$ -by- $N$  discrete Fourier transform (DFT) matrix with  $\mathbf{F}_N^H \mathbf{F}_N = \mathbf{I}_N$  and  $\mathbf{h}_i^0$  is the zero-padded version of the vector  $\mathbf{h}_i$  with length  $N$ , i.e.,  $\mathbf{h}_i^0 =$

$[\mathbf{h}_i^T \mathbf{0}_{1 \times (N-L_i)}]^T$ . The OFDM block  $\mathbf{x}_{F,i}$  is given by

$$\mathbf{x}_{F,i} = \mathbf{F}_N \mathbf{x}_T(\Delta_i) = \mathbf{\Lambda}(\Delta_i) \mathbf{F}_N \mathbf{x}_T \quad (5)$$

where  $\mathbf{\Lambda}(\Delta_i) = \text{diag} \left( \left[ 1, e^{-j \frac{2\pi \Delta_i}{N}}, \dots, e^{-j \frac{2\pi \Delta_i}{N} (N-1)} \right] \right)$  and  $\mathbf{x}_F = \mathbf{F}_N \mathbf{x}_T$ . In other words, the cyclic delay in the time domain is converted into a phase factor in the frequency domain. By defining  $\mathbf{X} = \text{diag}(\mathbf{x}_F)$ , (4) can be expressed as

$$\mathbf{y}_F = \sum_{i=1}^M \mathbf{\Lambda}(\Delta_i) \mathbf{X} \mathbf{h}_{F,i} + \mathbf{n}_F. \quad (6)$$

### B. Proposed CDD-OFDM-IM

Unlike the conventional CDD-OFDM scheme, this mapping method is not only carried out by the modulated data symbols, but also by means of the cyclic delays in different antenna paths. Inspired by the IM concept, additional information bits are transmitted by the permutation of the cyclic delays. As shown in Fig. 1, a total of  $p$  information bits are divided into two parts: the first part containing  $p_1$  bits is mapped onto a discrete signal constellation to determine the data symbols that form the OFDM block to be transmitted; the second part containing  $p_2$  bits is used for permuting the cyclic delays. Let  $\mathbb{K} = \{\Delta_{k_1}, \Delta_{k_2}, \dots, \Delta_{k_M}\}$  denote the cyclic delays, where  $\Delta_{k_i}$  is the cyclic delay in the  $i$ -th antenna path, given by

$$\Delta_{k_i} = \Delta(k_i - 1) \quad (7)$$

with  $k_i \in \{1, 2, \dots, M\}$  and  $k_i \neq k_{i'}$  if  $i \neq i'$  for all  $i, i' = 1, 2, \dots, M$ . Taking  $M = 2$  as an example, there are two possible permutations of the cyclic delays:  $\mathbb{K} = \{0, \Delta\}$  (i.e.,  $k_1 = 1, k_2 = 2$ ) and  $\mathbb{K} = \{\Delta, 0\}$  (i.e.,  $k_1 = 2, k_2 = 1$ ). It is worth pointing out that introducing a phase factor equal to or greater than the minimum phase difference of the adopted constellation will result in ambiguity in signal detection. Considering  $C$ -ary phase shift keying (PSK) for simplicity, the delay spacing needs to satisfy  $1 \leq \Delta \leq N/C - 1$ . On the other hand, we note that given  $M$ , there are in total  $M!$  possible permutations of the cyclic delays. Therefore, the number of information bits carried by the permutation of the cyclic delays is given by

$$p_2 = \lfloor \log_2(M!) \rfloor \quad (8)$$

which implies that  $\mathbb{K}$  has  $2^{p_2}$  possible realizations. For the total number of information bits carried by the modulated data symbols, we have

$$p_1 = N \log_2(C). \quad (9)$$

Consequently, the spectral efficiency of the CDD-OFDM-IM scheme is given by

$$\text{SE}_{\text{CDD-OFDM-IM}} = \frac{p}{N+L} = \frac{N \log_2(C) + \lfloor \log_2(M!) \rfloor}{N+L} \quad (10)$$

bits per second per Hertz (bps/Hz).

### C. Conventional CDD-CPSC

Unlike the CDD-OFDM scheme, the delay spacing  $\Delta$  in the conventional CDD-CPSC scheme is designed to be

not less than the maximum channel delay spread to avoid ISI. Specifically, by defining  $\mathbf{P}_N^0 \triangleq \mathbf{I}_N$ , the input-output relationship in the time domain is given by

$$\mathbf{y}_T = \sum_{i=1}^M \mathbf{H}_i \mathbf{x}_T(\Delta_i) + \mathbf{n}_T = \sum_{i=1}^M \mathbf{H}_i \mathbf{P}_N^{\Delta_i} \mathbf{x}_T + \mathbf{n}_T \quad (11)$$

where  $\Delta_i = \Delta(i-1)$ , and

$$\mathbf{H}_i = \begin{bmatrix} h_i(1) & \dots & 0 & \dots & h_i(2) \\ \vdots & \ddots & \vdots & \ddots & \vdots \\ h_i(L_i - 1) & \ddots & 0 & \ddots & h_i(L_i) \\ h_i(L_i) & \ddots & h_i(1) & \ddots & 0 \\ \vdots & \ddots & \vdots & \ddots & \vdots \\ 0 & \dots & h_i(L_i) & \dots & h_i(1) \end{bmatrix}.$$

We can rewrite (11) as the following equivalent expression

$$\mathbf{y}_T = \sum_{i=1}^M \mathbf{S} \mathbf{P}_N^{\Delta_i} \mathbf{h}_i^0 + \mathbf{n}_T = \mathbf{S} \mathbf{h}_T + \mathbf{n}_T$$

where

$$\mathbf{S} = \begin{bmatrix} s_1 & s_N & \dots & s_3 & s_2 \\ s_2 & s_1 & \dots & s_4 & s_3 \\ \vdots & \vdots & \ddots & \vdots & \vdots \\ s_{N-1} & s_{N-2} & \dots & s_1 & s_N \\ s_N & s_{N-1} & \dots & s_2 & s_1 \end{bmatrix}$$

and  $\mathbf{h}_T = \sum_{i=1}^M \mathbf{P}_N^{\Delta_i} \mathbf{h}_i^0$ . In other words, the cyclic delays on the symbol  $\mathbf{x}_T$  are converted into that of the corresponding channels. By letting  $\Delta = L$ ,  $\mathbf{h}_T$  is given by

$$\mathbf{h}_T = [\mathbf{h}_1^T, \mathbf{0}_{1 \times (L-L_1)}, \mathbf{h}_2^T, \mathbf{0}_{1 \times (L-L_2)}, \dots, \mathbf{h}_M^T, \mathbf{0}_{1 \times (L-L_M)}, \mathbf{0}_{1 \times (N-ML)}]^T \quad (12)$$

such that the multi-input single-output (MISO) channel degenerates to a single-input single-output (SISO) channel.

### D. Proposed CDD-CPSC-IM

Similar to the CDD-OFDM-IM scheme, the CDD-CPSC-IM system transmits additional information bits by means of the permutation of the cyclic delays in the antenna paths. Specifically, a total of  $p$  information bits are divided into two parts: the first part of  $p_1$  bits are mapped onto a discrete signal constellation to determine the data symbols  $\mathbf{x}_T$  to be transmitted; the second part of  $p_2$  bits are used for permuting the cyclic delays in the antenna paths. Assume that the cyclic delays in the antenna paths are given by

$$\Delta_{k_i} = \Delta(k_i - 1), i = 1, 2, \dots, M \quad (13)$$

where  $\{k_1, k_2, \dots, k_M\}$  is the permutation of the antenna indice. Unlike the conventional CDD-CPSC scheme in which  $\Delta = L$ , we let  $\Delta = \max\{L, \lfloor N/M \rfloor\}$  for the CDD-CPSC-IM scheme. Let us take  $L = 1$ ,  $M = 2$  and  $N = 4$  as an example, yielding  $\Delta = 2$ . There are two possible permutations:  $\{k_1 = 1, k_2 = 2\}$  and  $\{k_1 = 2, k_2 = 1\}$ . In other words, for  $\{k_1 = 1, k_2 = 2\}$ ,  $[s_1, s_2, s_3, s_4]^T$  and

$[s_3, s_4, s_1, s_2]^T$  are transmitted by the first and second TA, respectively; for  $\{k_1 = 2, k_2 = 1\}$ ,  $[s_3, s_4, s_1, s_2]^T$  and  $[s_1, s_2, s_3, s_4]^T$  are transmitted by the first and second TA, respectively; where  $\mathbf{x}_T = [s_1, s_2, s_3, s_4]^T$  is the data block to be transmitted with no delay. We note that the case of  $\{k_1 = 2, k_2 = 1\}$  with  $\mathbf{x}_T = [s_1, s_2, s_3, s_4]^T$  being the data block to be transmitted with no time delay is exactly the same as the case of  $\{k_1 = 1, k_2 = 2\}$  with  $\mathbf{x}_T = [s_3, s_4, s_1, s_2]^T$ . Therefore, in order to avoid ambiguity in signal detection, we consider the first data sample in the vector  $\mathbf{x}_T$  as an anchor point. Let us denote the data block with an anchor in the first sample point as  $\tilde{\mathbf{x}}_T = \mathbf{x}_T \odot [\mathbf{j}, \mathbf{1}_{1 \times (N-1)}]^T$ , where  $\mathbf{j} = \sqrt{-1}$  and  $\odot$  represents the Hadamard product. Therefore, the input-output relationship in the time domain is given by

$$\mathbf{y}_T = \sum_{i=1}^M \mathbf{H}_i \mathbf{P}_N^{\Delta_{k_i}} \tilde{\mathbf{x}}_T + \mathbf{n}_T \quad (14)$$

$$= \sum_{i=1}^M (\mathbf{S} \odot \mathbf{D}) \mathbf{P}_N^{\Delta_{k_i}} \mathbf{h}_i^0 + \mathbf{n}_T = \tilde{\mathbf{S}} \mathbf{h}_{T,\mathbb{K}} + \mathbf{n}_T \quad (15)$$

where  $\mathbf{D}$  is a diagonal matrix in which the main diagonal entries are  $\mathbf{j}$  and all off-diagonal entries are one,  $\tilde{\mathbf{S}} = \mathbf{S} \odot \mathbf{D}$ , and

$$\begin{aligned} \mathbf{h}_{T,\mathbb{K}} &= \sum_{i=1}^M \mathbf{P}_N^{\Delta_{k_i}} \mathbf{h}_i^0 \\ &= \left[ \mathbf{h}_{k_1}^T, \mathbf{0}_{1 \times (\Delta - L_{k_1})}, \mathbf{h}_{k_2}^T, \mathbf{0}_{1 \times (\Delta - L_{k_2})}, \dots, \mathbf{h}_{k_M}^T, \right. \\ &\quad \left. \mathbf{0}_{1 \times (\Delta - L_{k_M})}, \mathbf{0}_{1 \times (N - M\Delta)} \right]^T. \end{aligned} \quad (16)$$

It is worth pointing out that the CDD-CPSC-IM system is limited to using a number of transmit antennas which correspond with the ratio of the number of subcarriers to the length of the maximum channel delay spread, i.e.,  $M \leq N/L$ . Whereas the CDD-OFDM-IM system is limited to using a number of transmit antennas which correspond with the ratio of the number of subcarriers to the size of the signal constellation, i.e.,  $M \leq N/C$ . The number of information bits carried by the permutation of the cyclic delays is given by  $p_2 = \lfloor \log_2(M!) \rfloor$ , and the spectral efficiency of the CDD-CPSC-IM scheme is given by

$$\begin{aligned} \text{SE}_{\text{CDD-CPSC-IM}} &= \frac{p}{N + L} \\ &= \frac{N \log_2(C) + \lfloor \log_2(M!) \rfloor}{N + L} \text{ bps/Hz}. \end{aligned} \quad (17)$$

### III. EXTENSION OF CDD-OFDM-IM AND CDD-CPSC-IM

In this section, we present two methods to generate cyclic delay candidates for improving the SE performance of CDD-OFDM-IM and CDD-CPSC-IM systems.

#### A. Enhanced CDD-OFDM-IM Scheme

We note that the conventional CDD-OFDM system is limited to using a number of transmit antennas equal to that of sample points in the OFDM block. In practice, due to the high cost of radio frequency chains, the number of transmit

antennas is usually less than that of samples in the OFDM block (e.g.,  $N = 64$ ). Therefore, we exploit the fact of  $M < N$  by introducing an initial cyclic delay to each of the antenna paths, by which additional information bits are transmitted. Specifically, a total of  $p$  information bits are divided into three parts: the first part containing  $p_1$  bits is mapped onto a discrete signal constellation to determine the data symbols that form the OFDM block to be transmitted; the second part containing  $p_2$  bits is used for permuting the cyclic delays; and the third part containing  $p_3$  bits is used for determining the initial cyclic delay. Let  $\Delta_0$  denote the initial cyclic delay on the OFDM symbol. Then, the cyclic delay in the  $i$ -th antenna path is given by  $\Delta_0 + \Delta_{k_i}$ , where  $\Delta_{k_i}$  with  $i = 1, 2, \dots, M$  is given by (7). We note that the total delay spread between all of the antenna paths can be no more than the duration of the OFDM symbol, i.e.,  $\max_i \{\Delta_0 + \Delta_{k_i}\} - \min_i \{\Delta_0 + \Delta_{k_i}\} < N$ . Therefore, the initial cyclic delay can be no more than  $\min\{N - \Delta(M-1), N/C\}$ . In order to maximize the spectral efficiency, we let  $\Delta = 1$ , such that  $0 \leq \Delta_0 \leq \min\{N - M, N/C - 1\}$ . Consequently, the number of information bits carried by the initial cyclic delay is given by

$$p_3 = \lfloor \log_2(\min\{N - M + 1, N/C\}) \rfloor. \quad (18)$$

The number of additional information bits carried by the cyclic delays in the antenna paths is  $p_2 + p_3$  in total, and the spectral efficiency of the enhanced CDD-OFDM-IM (E-CDD-OFDM-IM) system is given by

$$\begin{aligned} \text{SE}_{\text{E-CDD-OFDM-IM}} &= \frac{N \log_2(C) + \lfloor \log_2(M!) \rfloor}{N + L} \\ &\quad + \frac{\lfloor \log_2(\min\{N - M + 1, N/C\}) \rfloor}{N + L} \text{ bps/Hz}. \end{aligned} \quad (19)$$

On the other hand, we note that the initial cyclic delay is limited by the minimum phase difference of the adopted signal constellation when  $C \geq N/(N - M + 1)$ . By relaxing the fixed delay interval condition, the total delay spread between all of the antenna paths can be extended to the duration of the OFDM symbol. Specifically, Let  $\mathbb{I} = \{\Delta_1, \Delta_2, \dots, \Delta_M\}$  denote the cyclic delays in increasing order, where  $\Delta_1 \in \{0, 1, \dots, \min\{N - M, N/C - 1\}\}$  and  $\Delta_i \in \{\Delta_{i-1} + 1, \dots, \min\{N - M + i, \Delta_{i-1} + N/C\} - 1\}$  with  $i = 2, \dots, M$ . Apparently,  $\mathbb{I}$  has more possible realizations than the initial cyclic delay, so that more additional information bits can be transmitted. This method is referred to as E-CDD-OFDM-IM 2 in the simulations.

#### B. Enhanced CDD-CPSC-IM Scheme

In order to improve the spectral efficiency of the CDD-CPSC-IM system, the equivalent SISO channel  $\mathbf{h}_{T,\mathbb{K}}$  of length  $N$  is split into  $M$  subblock. Each subblock of length  $\Delta$  is given by  $\mathbf{h}_{T,\mathbb{K},i} = \left[ \mathbf{h}_{k_1}^T, \mathbf{0}_{1 \times (\Delta - L_{k_1})} \right]^T$  with  $i = 1, 2, \dots, M$ . For each subblock, an initial cyclic delay is introduced, by which additional information bits are transmitted. Specifically, a total of  $p$  information bits are divided into three parts: the first part containing  $p_1$  bits is mapped onto a discrete signal

constellation to determine the data symbols that form the OFDM block to be transmitted; the second part containing  $p_2$  bits is used for permuting the cyclic delays; and the third part containing  $p_3$  bits is used for determining the initial cyclic delays in the antenna paths. Let us denote  $\Delta_{0,i}$  as the initial cyclic delay in the  $i$ -th antenna path, then we have the corresponding subblock given by

$$\tilde{\mathbf{h}}_{\mathbb{K},i} = \left[ \mathbf{0}_{1 \times \Delta_{0,i}}, \mathbf{h}_{k_1}^T, \mathbf{0}_{1 \times (\Delta - L_{k_i} - \Delta_{0,i})} \right]^T. \quad (20)$$

From (20), we see that the initial cyclic delays can take values from the interval  $[0, \Delta - L_{k_i}]$ . Therefore, the number of information bits carried by the initial cyclic delays is given by

$$p_4 = M \lfloor \log_2(\Delta - L + 1) \rfloor. \quad (21)$$

The number of additional information bits carried by the cyclic delays in the antenna paths is  $p_2 + p_4$  in total, and the spectral efficiency of the enhanced CDD-CPSC-IM (E-CDD-CPSC-IM) system is given by

$$\text{SE}_{\text{E-CDD-CPSC-IM}} = \frac{N \log_2(C) + \lfloor \log_2(M!) \rfloor}{N + L} + \frac{M \lfloor \log_2(\Delta - L + 1) \rfloor}{N + L} \text{ bps/Hz}. \quad (22)$$

Since the cyclic delay in the  $i$ -th antenna path is

$$\Delta_i = \Delta_{k_i} + \Delta_{0,i} \quad (23)$$

the equivalent SISO channel is given by

$$\tilde{\mathbf{h}}_{\mathbb{K}} = \left[ \mathbf{0}_{1 \times \Delta_{0,1}}, \mathbf{h}_{k_1}^T, \mathbf{0}_{1 \times (\Delta - L_{k_1} - \Delta_{0,1} + \Delta_{0,2})}, \dots, \mathbf{h}_{k_M}^T, \mathbf{0}_{1 \times (N - M\Delta - L_{k_M} - \Delta_{0,M})} \right]^T. \quad (24)$$

## IV. RECEIVER DESIGN AND PERFORMANCE ANALYSIS

### A. Receiver Design

1) *ML Receiver for CDD-OFDM-IM*: At the receiver, after removing the CP and performing the  $N$ -point FFT, the received block in the frequency domain is given by

$$\begin{aligned} \mathbf{y}_{\text{F}}^{\text{CDD-OFDM-IM}} &= \sum_{i=1}^M \mathbf{\Lambda}(\Delta_{k_i}) \mathbf{X} \mathbf{h}_{\text{F},i} + \mathbf{n}_{\text{F}} \\ &= \mathbf{X} \sum_{i=1}^M \mathbf{\Lambda}(\Delta_{k_i}) \mathbf{h}_{\text{F},i} + \mathbf{n}_{\text{F}}. \end{aligned} \quad (25)$$

For the conventional CDD scheme, the phase factors caused by the cyclic delays are known by the receiver and thus can be perfectly removed via channel equalization before signal detection. However, in the CDD-OFDM-IM scheme, the phase factors carry the information to be retrieved. In other words, the receiver needs to detect both the cyclic delay/phase factor in each antenna path and the constellation symbols. By searching for all possible permutations of the cyclic delays and the signal constellation points, the optimal ML detector makes a joint decision on the permutation of the cyclic delays and

the modulated symbols by minimizing the Euclidean distance, as follows:

$$\left( \hat{\mathbb{K}}, \hat{\mathbf{x}}_{\text{F}} \right) = \arg \min_{\mathbb{K}, \mathbf{x}_{\text{F}}} \left\| \mathbf{y}_{\text{F}}^{\text{CDD-OFDM-IM}} - \mathbf{X} \sum_{i=1}^M \mathbf{\Lambda}(\Delta_{k_i}) \mathbf{h}_{\text{F},i} \right\|^2. \quad (26)$$

We note that given any  $\mathbb{K}$ , (26) can be simplified to

$$\hat{\mathbf{x}}_{\text{F},\mathbb{K}} = \arg \min_{\mathbf{x}_{\text{F}}} \left\| \mathbf{y}_{\text{F}}^{\text{CDD-OFDM-IM}} - \mathbf{x}_{\text{F}} \odot \mathbf{h}_{\text{F},\mathbb{K}} \right\|^2 \quad (27)$$

$$= \arg \min_{\mathbf{x}_{\text{F}}} \left\| \text{diag}(\mathbf{h}_{\text{F},\mathbb{K}})^{-1} \mathbf{y}_{\text{F}}^{\text{CDD-OFDM-IM}} - \mathbf{x}_{\text{F}} \right\|^2 \quad (28)$$

where  $\mathbf{h}_{\text{F},\mathbb{K}} = \sum_{i=1}^M \mathbf{\Lambda}(\Delta_{k_i}) \mathbf{h}_{\text{F},i}$ . Due to the independence between the subcarriers, each symbol in (27) can be decoded independently.

2) *ML Receiver for CDD-CPSC-IM*: Let us define  $\mathbf{h}_{\text{T},\mathbb{K}} = [\underline{h}_1, \underline{h}_2, \dots, \underline{h}_N]^T$ . We can rewrite (15) as

$$\mathbf{y}_{\text{T}} = \underline{\mathbf{H}}_{\text{T},\mathbb{K}} \mathbf{x}_{\text{T}} \odot [j, \mathbf{1}_{1 \times (N-1)}]^T + \mathbf{n}_{\text{T}} \quad (29)$$

where

$$\underline{\mathbf{H}}_{\text{T},\mathbb{K}} = \begin{bmatrix} \underline{h}_1 & \underline{h}_N & \dots & \underline{h}_3 & \underline{h}_2 \\ \underline{h}_2 & \underline{h}_1 & \dots & \underline{h}_4 & \underline{h}_3 \\ \vdots & \vdots & \ddots & \vdots & \vdots \\ \underline{h}_{N-1} & \underline{h}_{N-2} & \dots & \underline{h}_1 & \underline{h}_N \\ \underline{h}_N & \underline{h}_{N-1} & \dots & \underline{h}_2 & \underline{h}_1 \end{bmatrix}. \quad (30)$$

The optimal ML detector jointly determines the permutation of the cyclic delays and the constellation symbols by searching for all possible permutations of the cyclic delays and the signal constellation points (to minimize the Euclidean distance), as shown below:

$$\left( \hat{\mathbb{K}}, \hat{\mathbf{x}}_{\text{T}} \right) = \arg \min_{\mathbb{K}, \mathbf{x}_{\text{T}}} \left\| \mathbf{y}_{\text{T}} - \underline{\mathbf{H}}_{\text{T},\mathbb{K}} \mathbf{x}_{\text{T}} \odot [j, \mathbf{1}_{1 \times (N-1)}]^T \right\|^2. \quad (31)$$

We note that since the  $N$  constellation symbols and  $\mathbb{K}$  respectively have  $C^N = 2^{p_1}$  and  $2^{p_2}$  possible realizations, the search complexity in (31) is of order  $C^N 2^{p_2} = 2^p$ .

3) *Low-complexity Receiver for CDD-CPSC-IM*: To reduce the high computational complexity of the optimal ML detection due to the involved FFT operations, we further propose a symbol-wise low-complexity receiver for the CDD-CPSC-IM system, which detects the IM and symbol bits sequentially. Specifically, given  $\mathbb{K}$ , some linear equalizations (such as the zero-forcing (ZF) and minimum mean square error (MMSE) equalizations can be applied before decoding the transmitted block  $\mathbf{x}_{\text{T}}$ . After performing ZF equalization, which is given by  $\mathbf{v}_{\text{ZF}} = \underline{\mathbf{H}}_{\text{T},\mathbb{K}}^{-1} \mathbf{y}_{\text{T}}$ , the output of the ZF equalizer is given by

$$\begin{aligned} \tilde{\mathbf{x}}_{\text{ZF},\mathbb{K}} &= \underline{\mathbf{H}}_{\text{T},\mathbb{K}}^{-1} \mathbf{y}_{\text{T}} \odot [-j, \mathbf{1}_{1 \times (N-1)}]^T \\ &= \mathbf{x}_{\text{T}} + \underline{\mathbf{H}}_{\text{T},\mathbb{K}}^{-1} \mathbf{n}_{\text{T}} \odot [-j, \mathbf{1}_{1 \times (N-1)}]^T. \end{aligned} \quad (32)$$

Although the linear ZF receiver is simple, the MMSE equalization, which is given by

$$\mathbf{v}_{\text{MMSE}} = \left( \underline{\mathbf{H}}_{\text{T},\mathbb{K}}^H \underline{\mathbf{H}}_{\text{T},\mathbb{K}} + \frac{1}{\rho} \mathbf{I}_N \right)^{-1} \underline{\mathbf{H}}_{\text{T},\mathbb{K}}^H \mathbf{y}_{\text{T}} \quad (33)$$

$$\begin{aligned}
\tilde{\mathbf{E}} &= E \left\{ \begin{bmatrix} \mathbf{F}_N \mathbf{h}_1^0 (\mathbf{h}_1^0)^H \mathbf{F}_N^H & \mathbf{F}_N \mathbf{h}_1^0 (\mathbf{h}_2^0)^H \mathbf{F}_N^H & \dots & \mathbf{F}_N \mathbf{h}_1^0 (\mathbf{h}_M^0)^H \mathbf{F}_N^H \\ \mathbf{F}_N \mathbf{h}_2^0 (\mathbf{h}_1^0)^H \mathbf{F}_N^H & \mathbf{F}_N \mathbf{h}_2^0 (\mathbf{h}_2^0)^H \mathbf{F}_N^H & \dots & \mathbf{F}_N \mathbf{h}_2^0 (\mathbf{h}_M^0)^H \mathbf{F}_N^H \\ \vdots & \vdots & \ddots & \vdots \\ \mathbf{F}_N \mathbf{h}_M^0 (\mathbf{h}_1^0)^H \mathbf{F}_N^H & \mathbf{F}_N \mathbf{h}_M^0 (\mathbf{h}_2^0)^H \mathbf{F}_N^H & \dots & \mathbf{F}_N \mathbf{h}_M^0 (\mathbf{h}_M^0)^H \mathbf{F}_N^H \end{bmatrix} \right\} \\
&\stackrel{(a)}{=} \begin{bmatrix} \mathbf{F}_N E \left\{ \mathbf{h}_1^0 (\mathbf{h}_1^0)^H \right\} \mathbf{F}_N^H & \mathbf{0}_{N \times N} & \dots & \mathbf{0}_{N \times N} \\ \mathbf{0}_{N \times N} & \mathbf{F}_N E \left\{ \mathbf{h}_2^0 (\mathbf{h}_2^0)^H \right\} \mathbf{F}_N^H & \dots & \mathbf{0}_{N \times N} \\ \vdots & \vdots & \ddots & \vdots \\ \mathbf{0}_{N \times N} & \mathbf{0}_{N \times N} & \dots & \mathbf{F}_N E \left\{ \mathbf{h}_M^0 (\mathbf{h}_M^0)^H \right\} \mathbf{F}_N^H \end{bmatrix} \\
&= \begin{bmatrix} \mathbf{F}_N \mathbf{E}_1 \mathbf{F}_N^H & \mathbf{0}_{N \times N} & \dots & \mathbf{0}_{N \times N} \\ \mathbf{0}_{N \times N} & \mathbf{F}_N \mathbf{E}_2 \mathbf{F}_N^H & \dots & \mathbf{0}_{N \times N} \\ \vdots & \vdots & \ddots & \vdots \\ \mathbf{0}_{N \times N} & \mathbf{0}_{N \times N} & \dots & \mathbf{F}_N \mathbf{E}_M \mathbf{F}_N^H \end{bmatrix} \tag{42}
\end{aligned}$$

where (a) is obtained due to the mutual independence of the channels  $\mathbf{h}_i$ 's, and  $\mathbf{E}_i = \begin{bmatrix} \frac{1}{L_i} \mathbf{I}_{L_i} & \mathbf{0}_{L_i \times (N-L_i)} \\ \mathbf{0}_{(N-L_i) \times L_i} & \mathbf{0}_{L_i \times L_i} \end{bmatrix}$ .

can take advantage of the diversity of the CDD-CPSC systems. The output of the MMSE equalizer is given by

$$\tilde{\mathbf{x}}_{\text{MMSE},\mathbb{K}} = \left( \underline{\mathbf{H}}_{\text{T},\mathbb{K}}^H \underline{\mathbf{H}}_{\text{T},\mathbb{K}} + \frac{1}{\rho} \mathbf{I}_N \right)^{-1} \underline{\mathbf{H}}_{\text{T},\mathbb{K}}^H \mathbf{y}_{\text{T}} \odot [-j, \mathbf{1}_{1 \times (N-1)}]^T. \tag{34}$$

At high SNR, (34) can be simplified to

$$\tilde{\mathbf{x}}_{\text{MMSE},\mathbb{K}} = \mathbf{x}_{\text{T}} + \left( \underline{\mathbf{H}}_{\text{T},\mathbb{K}}^H \underline{\mathbf{H}}_{\text{T},\mathbb{K}} \right)^{-1} \underline{\mathbf{H}}_{\text{T},\mathbb{K}}^H \mathbf{n}_{\text{T}} \odot [-j, \mathbf{1}_{1 \times (N-1)}]^T. \tag{35}$$

Both of the vectors  $\tilde{\mathbf{x}}_{\text{ZF},\mathbb{K}}$  and  $\tilde{\mathbf{x}}_{\text{MMSE},\mathbb{K}}$  are sufficient statistics to detect  $\mathbf{x}_{\text{T}}$  from  $\mathbf{y}_{\text{T}}$ . Let  $\tilde{\mathbf{x}}_{\mathbb{K}} \triangleq [\tilde{s}_{\mathbb{K},1}, \tilde{s}_{\mathbb{K},2}, \dots, \tilde{s}_{\mathbb{K},N}]^T$  denote the output of the linear equalizer. Then, each symbol in  $\tilde{\mathbf{x}}_{\mathbb{K}}$  is demodulated independently, i.e.,

$$\hat{s}_{\mathbb{K},i} = \arg \min_{s \in \mathbb{C}} |\tilde{s}_{\mathbb{K},i} - s|^2 \tag{36}$$

where  $\hat{s}_{\mathbb{K},i}$  denotes the hard decision on  $\tilde{s}_{\mathbb{K},i}$  and  $\mathbb{C}$  contains all possible constellation points. Then the estimate of  $\mathbb{K}$  is given by

$$\hat{\mathbb{K}} = \arg \min_{\mathbb{K}} \left\| \mathbf{y}_{\text{T}} - \underline{\mathbf{H}}_{\text{T},\mathbb{K}} \hat{\mathbf{x}}_{\text{T},\mathbb{K}} \odot [j, \mathbf{1}_{1 \times (N-1)}]^T \right\|^2 \tag{37}$$

where  $\hat{\mathbf{x}}_{\text{T},\mathbb{K}} \triangleq [\hat{s}_{\mathbb{K},1}, \hat{s}_{\mathbb{K},2}, \dots, \hat{s}_{\mathbb{K},N}]^T$ , and the estimate of  $\mathbf{x}_{\text{T}}$  is given by  $\hat{\mathbf{x}}_{\text{T}} = \hat{\mathbf{x}}_{\text{T},\hat{\mathbb{K}}}$ . The search complexity of this symbol-wise low-complexity receiver is of order  $CN2^{p^2}$ .

## B. Performance Analysis

In this section, we characterize the average bit error probability (ABEP) and the coding gain of the CDD-OFDM-IM scheme using the ML detector in (26), which are also the lower bounds to the CDD-CPSC-IM scheme with the ML detection. We define  $\rho \triangleq E_b/N_0$  as the SNR with  $E_b = (N+L)/p$  being the average transmitted energy per bit.

1) *Average Bit Error Probability:* We use the following matrix notation for the input-output relationship in (25)

$$\mathbf{y}_{\text{F}}^{\text{CDD-OFDM-IM}} = \mathbf{W} \mathbf{h}_{\text{F}} + \mathbf{n}_{\text{F}} \tag{38}$$

where  $\mathbf{W} = \mathbf{X} [\Lambda(\Delta_{k_1}), \dots, \Lambda(\Delta_{k_M})] = \mathbf{X} \bar{\mathbf{A}}$  and  $\mathbf{h}_{\text{F}} = \begin{bmatrix} \mathbf{h}_{\text{F},1} \\ \vdots \\ \mathbf{h}_{\text{F},M} \end{bmatrix}$ . If  $\mathbf{W}$  is transmitted and it is erroneously detected as  $\hat{\mathbf{W}}$ , the conditional pairwise error probability (PEP) expression for this model is given by

$$P(\mathbf{W} \rightarrow \hat{\mathbf{W}} | \mathbf{h}_{\text{F}}) = Q \left( \sqrt{\frac{\delta}{2N_0}} \right) \tag{39}$$

where  $\delta = \left\| (\mathbf{W} - \hat{\mathbf{W}}) \mathbf{h}_{\text{F}} \right\|^2 = \mathbf{h}_{\text{F}}^H \mathbf{A} \mathbf{h}_{\text{F}}$  with  $\mathbf{A} = (\mathbf{W} - \hat{\mathbf{W}})^H (\mathbf{W} - \hat{\mathbf{W}})$ . We use the following approximation of the Gaussian  $Q$ -function

$$Q(x) \cong \frac{1}{12} \exp(-x^2/2) + \frac{1}{4} \exp(-2x^2/3). \tag{40}$$

Then, the unconditional PEP is obtained by

$$P(\mathbf{W} \rightarrow \hat{\mathbf{W}}) \cong E_{\mathbf{h}_{\text{F}}} \left\{ \frac{1}{12} \exp(-q_1 \delta) + \frac{1}{4} \exp(-q_2 \delta) \right\} \tag{41}$$

where  $q_1 = 1/(4N_0)$  and  $q_2 = 1/(3N_0)$ . To calculate the expectation in (41), we define  $\tilde{\mathbf{E}} = E \{ \mathbf{h}_{\text{F}} \mathbf{h}_{\text{F}}^H \}$ , which can be calculated as (42), shown at the top of the page. Based on the probability density function of  $\mathbf{h}_{\text{F}}$  given as

$$f(\mathbf{h}_{\text{F}}) = \frac{\pi^{-MN}}{\det(\tilde{\mathbf{K}})} \exp \left( -\mathbf{h}_{\text{F}}^H \tilde{\mathbf{K}}^{-1} \mathbf{h}_{\text{F}} \right) \tag{43}$$

the unconditional PEP in (41) is given by

$$P(\mathbf{W} \rightarrow \hat{\mathbf{W}}) \cong \frac{1/12}{\det(\mathbf{I}_{MN} + q_1 \tilde{\mathbf{K}}\mathbf{A})} + \frac{1/4}{\det(\mathbf{I}_{MN} + q_2 \tilde{\mathbf{K}}\mathbf{A})}. \quad (44)$$

Based on (44), the ABEP of the OFDM-CDD-IM scheme can be evaluated by

$$P_b \approx \frac{1}{2^p} \sum_{\mathbf{W}} \sum_{\hat{\mathbf{W}}} P(\mathbf{W} \rightarrow \hat{\mathbf{W}}) \frac{e(\mathbf{W}, \hat{\mathbf{W}})}{p} \quad (45)$$

where  $e(\mathbf{W}, \hat{\mathbf{W}})$  denotes the number of bit errors for the pairwise error event  $(\mathbf{W} \rightarrow \hat{\mathbf{W}})$ .

2) *Coding Gain*: We define  $\mathbf{C}_\alpha = \mathbf{I}_{MN} + q_\alpha \tilde{\mathbf{K}}\mathbf{A} = \mathbf{I}_{MN} + q_\alpha \mathbf{B}$  with  $\alpha = 1, 2$ . Then, we have

$$\det(\mathbf{C}_\alpha) = \prod_{j=1}^{MN} \lambda_j(\mathbf{C}_\alpha) = \prod_{j=1}^r (1 + q_\alpha \lambda_j(\mathbf{B})) \quad (46)$$

where  $\lambda_j(\cdot)$  represents the  $j$ -th eigenvalue of a matrix, and  $r = \text{rank}(\mathbf{B}) \leq \min(\text{rank}(\tilde{\mathbf{K}}), \text{rank}(\mathbf{A}))$ . For large enough SNR, we have  $q_\alpha \gg 1$ , so that the above determinant can be approximated as:  $\det(\mathbf{C}_\alpha) \simeq q_\alpha^r \prod_{j=1}^r \lambda_j(\mathbf{B})$ ; and (44) can be rewritten as

$$\begin{aligned} P(\mathbf{W} \rightarrow \hat{\mathbf{W}}) &\simeq \left( 12q_1^r \prod_{j=1}^r \lambda_j(\mathbf{B}) \right)^{-1} + \left( 4q_2^r \prod_{j=1}^r \lambda_j(\mathbf{B}) \right)^{-1} \\ &= \left( \prod_{j=1}^r \lambda_j(\mathbf{B}) \right)^{-1} \left( \frac{4^r}{12} + \frac{3^r}{4} \right) N_0^r. \end{aligned} \quad (47)$$

We can conclude from (47) that the diversity order of the OFDM-CDD-IM system is determined by  $r$ , which can take values from the interval  $[1, MN]$ . For larger  $r$ , the unconditional PEP in (47) decays faster with SNR. This means that at high SNR, the higher order terms with  $r > 1$  in (45) can be neglected and the ABEP is determined by the terms of order  $r = 1$ . We note that  $r = \text{rank}(\mathbf{A}) = 1$  when the receiver correctly detects the cyclic delays in the antenna paths and makes a single decision error out of  $N$  constellation symbols. When  $r = 1$ , (47) can be simplified as

$$P(\mathbf{W} \rightarrow \tilde{\mathbf{W}}) \simeq \frac{13}{12} \lambda_1^{-1}(\mathbf{B}) N_0 \quad (48)$$

where  $\tilde{\mathbf{W}}$  represents an error detection with only one single symbol decision error. Moreover, the conditional PEP of the only single error decision on the  $n$ -th constellation symbol is defined as  $P(\mathbf{W} \rightarrow \tilde{\mathbf{W}}|n)$ , where  $n$  takes values from the interval  $[1, N]$ . Then, the ABEP of the only single error decision on the  $n$ -th constellation symbol can be evaluated as

$$P_b(n) = \frac{N}{p} \frac{1}{2^p} \sum_{\mathbf{W}} \sum_{\tilde{\mathbf{W}}} P(\mathbf{W} \rightarrow \tilde{\mathbf{W}}|n) e(\mathbf{W}, \tilde{\mathbf{W}}) \quad (49)$$

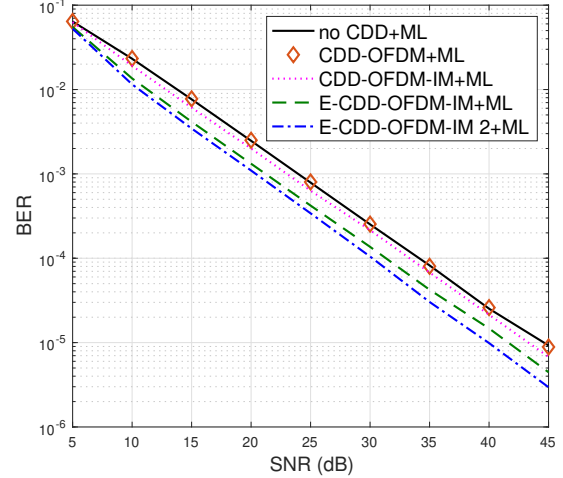


Fig. 2. Performance comparison between OFDM without CDD, conventional CDD-OFDM, CDD-OFDM-IM, and enhanced CDD-OFDM-IM schemes.

and the asymptotic ABEP of the OFDM-CDD-IM scheme can be approximated as

$$P_b \approx \frac{1}{N} \sum_{n=1}^N P_b(n). \quad (50)$$

We note that the conventional CDD where the receiver knows a priori the cyclic delays in the antenna paths is a special case of the OFDM-CDD-IM scheme with  $p = p_1$ . Therefore, the asymptotic ABEP of the CDD scheme can be expressed by (50) as well. At the same SNR, the ratio of the ABEP of the OFDM-CDD-IM scheme to that of the conventional CDD scheme is given by

$$\nu = \frac{N/p}{N/p_1} \cdot \frac{N_0}{(p/p_1)N_0} = \frac{p_1^2}{(p_1 + p_2)^2}. \quad (51)$$

Therefore, the coding gain achieved by the OFDM-CDD-IM scheme is  $R = 1/\nu = (p/p_1)^2$ . From (51), it can be observed that the coding gain is contributed by the ratio of the number of bits carried on each subcarrier and the ratio of the noise variances.

## V. SIMULATION RESULTS

In this section, numerical simulation results are provided to evaluate the performance of the CDD-OFDM-IM and CDD-CPSC-IM systems as well as validate the theory analysis in Section IV-B. The bit error rate (BER) is chosen as the performance metric. Binary phase shift keying (BPSK) modulation is used. The number of sample points or time slots in each block is  $N = 8$ . We assume that all channels have the same number of taps in time domain for simplicity. We set  $L_1 = L_2 = 3$ , and the CP length is  $L = 3$ . The number of transmit antennas is  $M = 2$ . The pure CDD-OFDM and CDD-CPSC schemes without IM are taken as benchmark schemes for comparison. The OFDM and CPSC transmissions without CDD are also considered as benchmarks for comparison, in which each transmit antenna sends the same data streams. In other words, there is no delay between the transmit antennas.

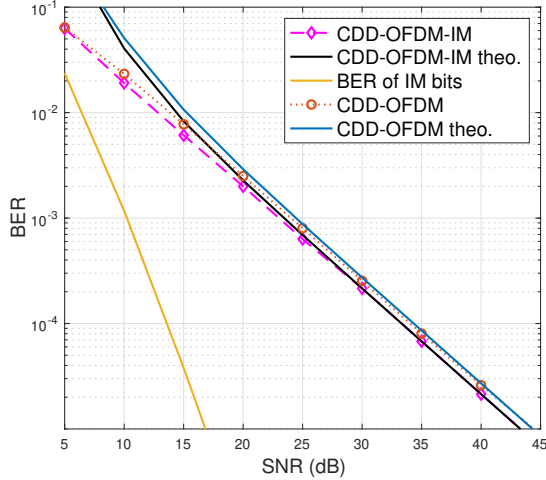


Fig. 3. Comparison between conventional CDD-OFDM and CDD-OFDM-IM with ML detection.

We compare in Fig. 2 the performance of the CDD-OFDM-IM and two enhanced CDD-OFDM-IM schemes with the benchmark schemes. We can see that the pure CDD-OFDM without IM achieves almost the same BER performance as the OFDM transmission without CDD, while the family of CDD-OFDM with IM achieves a significant BER gain over them. In particular, the enhanced CDD-OFDM-IM 2 achieves about 3.5 dB SNR gain over the pure CDD-OFDM scheme without IM. As seen from Fig. 3, the CDD-OFDM-IM scheme achieves about 1 dB SNR gain over the pure CDD-OFDM scheme without IM, which corroborates the accuracy of the analytical coding gain as  $10 \log_{10}(R) = 20 \log_{10}(p/p_1) = 1.0231$  dB. On the other hand, the error rate of the IM bits decays with SNR much faster than that of the constellation symbol bits which determines the BER of the CDD-OFDM-IM scheme at high SNR. This is expected since the information carried by IM has higher reliability such that can be used to broadcast control signaling.

The performance comparison between the CPSC transmission without CDD, CDD-CPSC without IM, CDD-CPSC-IM, and enhanced CDD-CPSC-IM is provided in Figs. 4 and 5, where receivers employ ZF and MMSE equalizations, respectively. It can be observed in Fig. 4 that the BER performance of the CDD-CPSC-IM using a ZF equalizer is lower bounded by that of the CDD-OFDM-IM scheme. With the same ZF/MMSE receiver, the ABER performance of the CDD-CPSC-IM scheme is slightly better than that of the CDD-CPSC schemes without IM. Compared to the CDD-CPSC-IM scheme, the enhanced CDD-CPSC-IM scheme has a higher spectral efficiency, but its ABER performance is slightly worse. There is a trade-off between the system spectral efficiency and the ABER performance. On the other hand, the MMSE receiver is superior to the ZF receiver, especially at high SNR. This can be understood by the fact that the MMSE receiver is information lossless.

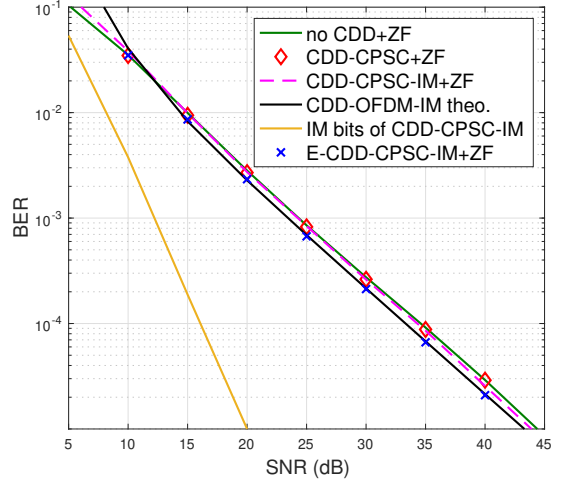


Fig. 4. Performance comparison between CPSC transmission without CDD, conventional CDD-CPSC, CDD-CPSC-IM, and enhanced CDD-CPSC-IM schemes with the ZF receiver.

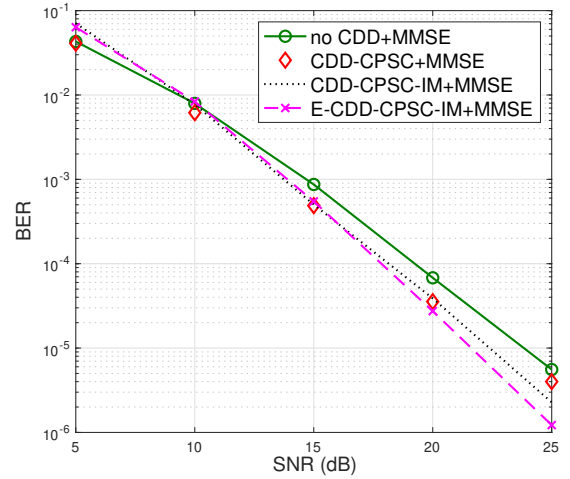


Fig. 5. Performance comparison between CPSC transmission without CDD, conventional CDD-CPSC, CDD-CPSC-IM, and enhanced CDD-CPSC-IM schemes with the MMSE receiver.

## VI. CONCLUSION

In this paper, we have proposed CDD-OFDM-IM and CDD-CPSC-IM to improve the SEs of CDD systems with OFDM and CPSC transmissions, respectively. The proposed schemes include the functions of both CDD and IM, thereby inheriting both advantages. Optimal and/or suboptimal low-complexity receivers have been designed for the CDD-OFDM-IM and CDD-CPSC-IM systems. The BER performance of both proposed systems has been further evaluated with theoretically derived upper bounds, and been compared with that of pure CDD-OFDM and CDD-CPSC systems without IM. Simulation results have verified the accuracy of the analysis and the advantages of the proposed systems.

## REFERENCES

- [1] A. Dammann and S. Kaiser, "Standard conformable antenna diversity techniques for OFDM and its application to the DVB-T system," in *Proc. IEEE GLOBECOM*, San Antonio, TX, USA, Nov. 2001, pp. 388–397.
- [2] K. J. Kim, M. Di Renzo, H. Liu, P. V. Orlik, and H. V. Poor, "Performance analysis of distributed single carrier systems with distributed cyclic delay diversity," *IEEE Trans. Commun.*, vol. 65, no. 12, pp. 5514–5528, Dec. 2017.
- [3] G. Auer, "Channel estimation by set partitioning for OFDM with cyclic delay diversity," in *Proc. IEEE Vehicular Technology Conference (VTC)*, Los Angeles, CA, USA, Sep. 2004, pp. 669–673.
- [4] G. Bauch, "Differential modulation and cyclic delay diversity in orthogonal frequency-division multiplex," *IEEE Trans. Commun.*, vol. 54, no. 5, pp. 798–801, May 2006.
- [5] J. Tan and G. L. Stuber, "Multicarrier delay diversity modulation for MIMO systems," *IEEE Trans. Wireless Commun.*, vol. 3, no. 5, pp. 1756–1763, Sep. 2004.
- [6] G. Bauch and J. S. Malik, "Cyclic delay diversity with bit-interleaved coded modulation in orthogonal frequency division multiple access," *IEEE Trans. Wireless Commun.*, vol. 5, no. 8, pp. 2092–2100, Aug. 2006.
- [7] A. H. Mehana and A. Nosratinia, "Single-carrier frequency-domain equalizer with multi-antenna transmit diversity," *IEEE Trans. Wireless Commun.*, vol. 12, no. 1, pp. 388–397, Jan. 2013.
- [8] Y.-C. Liang, W. S. Leon, Y. Zeng, and C. Xu, "Design of cyclic delay diversity for single carrier cyclic prefix (SCCP) transmissions with block-iterative GDFE (BI-GDFE) receiver," *IEEE Trans. Wireless Commun.*, vol. 7, no. 2, pp. 677–684, Feb. 2008.
- [9] U. K. Kwon and G. H. Im, "Cyclic delay diversity with frequency domain turbo equalization for uplink fast fading channels," *IEEE Commun. Lett.*, vol. 13, no. 3, pp. 184–186, Mar. 2009.
- [10] A. Tajer and A. Nosratinia, "Diversity order in ISI channels with single-carrier frequency-domain equalizers," *IEEE Trans. Wireless Commun.*, vol. 9, no. 3, pp. 1022–1032, Mar. 2010.
- [11] K. J. Kim, H. Liu, M. Wen, M. Di Renzo, and H. V. Poor, "Outage probability analysis of spectrum sharing systems with distributed cyclic delay diversity," *IEEE Trans. Commun.*, vol. 67, no. 6, pp. 4435–4449, Jun. 2019.
- [12] K. J. Kim, M. Di Renzo, H. Liu, T. A. Tsiftsis, P. V. Orlik, and H. Vincent Poor, "Distributed cyclic delay diversity systems with spatially distributed interferers," *IEEE Trans. Wireless Commun.*, vol. 18, no. 4, pp. 2066–2079, Apr. 2019.
- [13] K. J. Kim, H. Liu, M. Wen, P. V. Orlik, and H. V. Poor, "Secrecy performance analysis of distributed asynchronous cyclic delay diversity-based cooperative single carrier systems," *IEEE Trans. Commun.*, vol. 68, no. 5, pp. 2680–2694, May 2020.
- [14] L. Zheng and D. Tse, "Diversity and multiplexing: a fundamental tradeoff in multiple-antenna channels," *IEEE Trans. Inf. Theory*, vol. 49, no. 5, pp. 1073–1096, May 2003.
- [15] S. D. Tusha, A. Tusha, E. Basar, and H. Arslan, "Multidimensional index modulation for 5G and beyond wireless networks," *Proc. IEEE*, to appear.
- [16] T. Mao, Q. Wang, Z. Wang, and S. Chen, "Novel index modulation techniques: A survey," *IEEE Commun. Survey & Tut.*, vol. 21, no. 1, pp. 315–348, 1st Quarter 2019.
- [17] X. Cheng, M. Zhang, M. Wen, and L. Yang, "Index modulation for 5G: Striving to do more with less," *IEEE Wireless Commun.*, vol. 25, no. 2, pp. 126–132, Apr. 2018.
- [18] E. Basar, M. Wen, R. Mesleh, M. Di Renzo, Y. Xiao, and H. Haas, "Index modulation techniques for next-generation wireless networks," *IEEE Access*, vol. 5, pp. 16693–16746, Sep. 2017.
- [19] M. Wen, X. Cheng, and L. Yang, *Index Modulation for 5G Wireless Communications*. Springer International Publishing AG, Cham, Switzerland, 2017.
- [20] N. Ishikawa, S. Sugiura, and L. Hanzo, "50 years of permutation, spatial and index modulation: From classic RF to visible light communications and data storage," *IEEE Commun. Survey & Tut.*, vol. 20, no. 3, pp. 1905–1938, 3rd Quarter 2018.
- [21] S. Dang, O. Amin, B. Shihada, and M.-S. Alouini, "What should 6G be?" *Nature Electronics*, vol. 3, no. 1, pp. 20–29, 2020.
- [22] D. Slepian, "Permutation modulation," *Proc. IEEE*, vol. 53, no. 3, pp. 228–236, Mar. 1965.
- [23] M. Wen, B. Zheng, K. J. Kim, M. Di Renzo, T. A. Tsiftsis, K.C. Chen, and N. Al-Dhahir, "A survey on spatial modulation in emerging wireless systems: Research progresses and applications," *IEEE J. Sel. Areas Commun.*, vol. 37, no. 9, pp. 1949–1972, Sep. 2019.
- [24] E. Basar, U. Aygolu, E. Panayirci, and H. V. Poor, "Orthogonal frequency division multiplexing with index modulation," *IEEE Trans. Signal Process.*, vol. 61, no. 22, pp. 5536–5549, Nov. 2013.
- [25] M. Wen, B. Ye, E. Basar, Q. Li, and F. Ji, "Enhanced orthogonal frequency division multiplexing with index modulation," *IEEE Trans. Wireless Commun.*, vol. 16, no. 7, pp. 4786–4801, Jul. 2017.
- [26] S. Gao, M. Zhang, and X. Cheng, "Precoded index modulation for multi-input multi-output OFDM," *IEEE Trans. Wireless Commun.*, vol. 17, no. 1, pp. 17–28, Jan. 2018.
- [27] Y. Bian, X. Cheng, M. Wen, L. Yang, H. V. Poor, and B. Jiao, "Differential spatial modulation," *IEEE Trans. Veh. Technol.*, vol. 64, no. 7, pp. 3262–3268, Jul. 2015.
- [28] S. Gao, X. Cheng, and L. Yang, "Spatial multiplexing with limited RF chains: Generalized beamspace modulation (GBM) for mmWave massive MIMO," *IEEE J. Sel. Areas Commun.*, vol. 37, no. 9, pp. 2029–2039, Sep. 2019.
- [29] M. Wen, E. Basar, Q. Li, B. Zheng, and M. Zhang, "Multiple-mode orthogonal frequency division multiplexing with index modulation," *IEEE Trans. Commun.*, vol. 65, no. 9, pp. 3892–3906, Sep. 2017.
- [30] M. Wen, Q. Li, E. Basar, and W. Zhang, "Generalized multiple-mode OFDM with index modulation," *IEEE Trans. Wireless Commun.*, vol. 17, no. 10, pp. 6531–6543, Oct. 2018.
- [31] M. Wen, X. Chen, Q. Li, E. Basar, Y.-C. Wu, and W. Zhang, "Index modulation aided subcarrier mapping for dual-hop OFDM relaying," *IEEE Trans. Commun.*, vol. 67, no. 9, pp. 6012–6024, Sep. 2019.
- [32] G. Auer, "Channel estimation for OFDM with cyclic delay diversity," in *Proc. IEEE International Symposium on Personal, Indoor and Mobile Radio Communications (PIMRC)*, Barcelona, Spain, Sep. 2004, pp. 1792–1796.
- [33] A. Dammann, "On antenna diversity techniques for OFDM systems," Ph.D. dissertation, Universität Ulm, Germany, Jun. 2005, VDI Verlag Düsseldorf, Series 10, No. 766.